# Supporting Information

## Facile fabrication of oxygen and carbon co-doped carbon nitride nanosheet for efficient visible light photocatalytic $H_2$ evolution and $CO_2$ reduction

Shipeng Wan[a,c], Man Ou[b,c]*, Xinming Wang[a,c], Yanan Wang[a,c], Yiqing Zeng[a,c], Jie Ding[a,c], Shule Zhang[a,c], Qin Zhong[a,c]*

[a]*School of Chemical Engineering, Nanjing University of Science and Technology, Nanjing, Jiangsu 210094, China*

[b]*School of Energy Science and Engineering, Nanjing Tech University, Nanjing, Jiangsu 211816, PR Chian*

[c]*Nanjing AIREP Environmental Protection Technology Co., Ltd., Nanjing, Jiangsu 210091, China*

**Corresponding author: Qin Zhong. Email: zq304@njust.edu.cn. Tel/Fax number: +86 25 84315517.*

Submitted to *Dalton Transactions*

June, 2019

**Fig. S1** (a**)** Photocatalytic experimental apparatus; (b-d) GC7900 gas chromatography calibration curves for CO, $CH_4$ and $H_2$.

**Fig. S2** The UV-Raman spectra spectra for GCN and $MG_x$ ($x$ = 1.0, 2.0, 3.0, 7.5, 15)

**Fig. S3** (a-b) SEM images of GCN, (c) The photo of GCN samples; (e-d) SEM images of $MG_{3.0}$, (f) The photo of $MG_{3.0}$ samples.

**Fig. S4** (a) TEM images of carbon nitride nanosheet $MG_{3.0}$ along with the energy-dispersive X-ray (EDX) spectrum.

**Fig. S5** (a) $H_2$ evolution for GCN, $MG_{3.0}$ without $HNO_3$ treatment, $MG_{3.0}$ with $HNO_3$ treatment; (b) $CO_2$ reduction for GCN, $MG_{3.0}$ without $HNO_3$ treatment, $MG_{3.0}$ with $HNO_3$ treatment.

**Fig. S6** (a) XRD patterns and (b) FTIR spectra of $MG_{3.0}$ before and after the photocatalytic $H_2$ generation.

**Table S1** Elemental contents and C/N atomic ratio of GCN and $MG_{3.0}$ by elemental analyzer.

**Table S2** Comparison of $H_2$ evolution rate for the carbon nitride nanosheet and reported carbon nitride base photocatalysts.

**Section S1** The procedure to achieve the valence band potential ($E_{VB}$) and conduction band potential ($E_{CB}$) values.

**Section S2** The discussion for the preferential formation of CO in the photocatalytic $CO_2$ reduction.

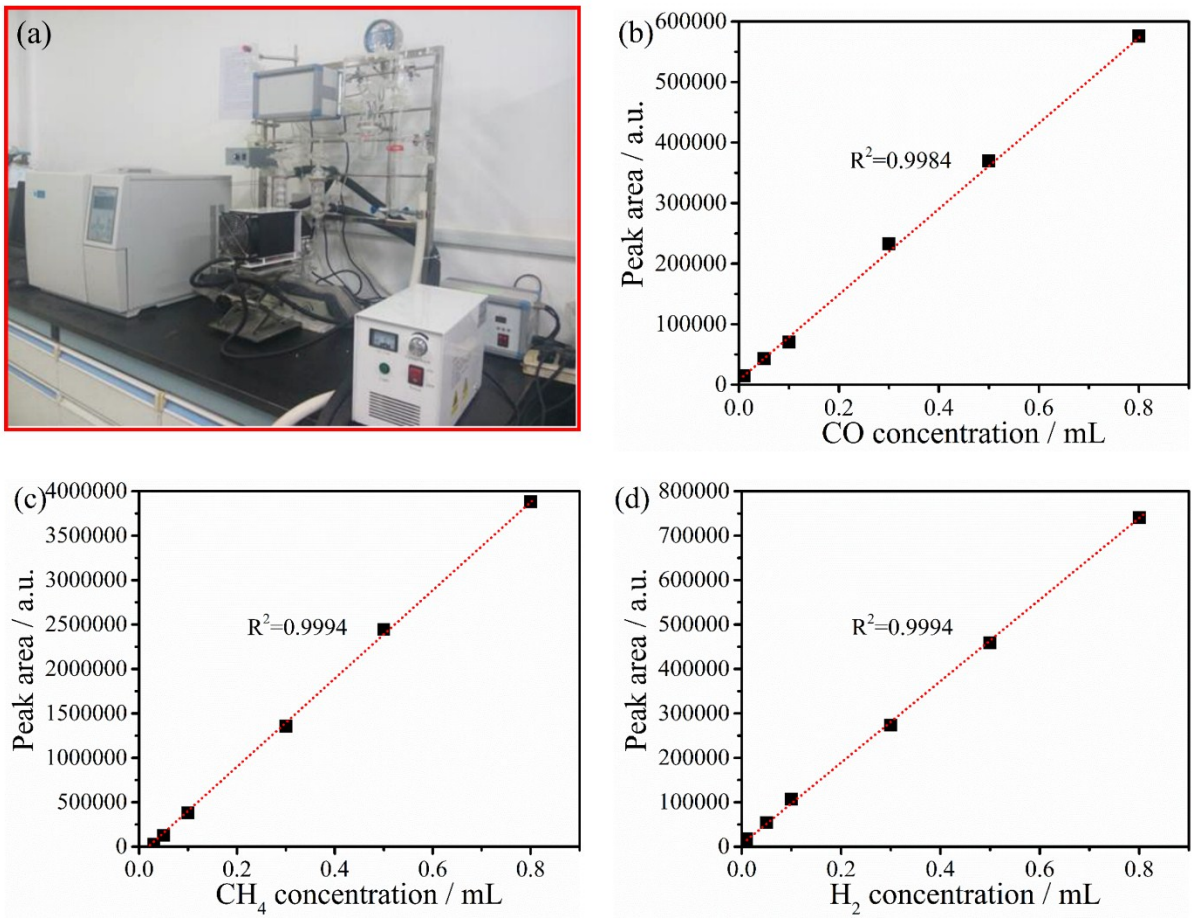


**Fig. S1** (a) Photocatalytic experimental apparatus; (b-d) GC7900 gas chromatography calibration curves for CO, $CH_4$ and $H_2$.

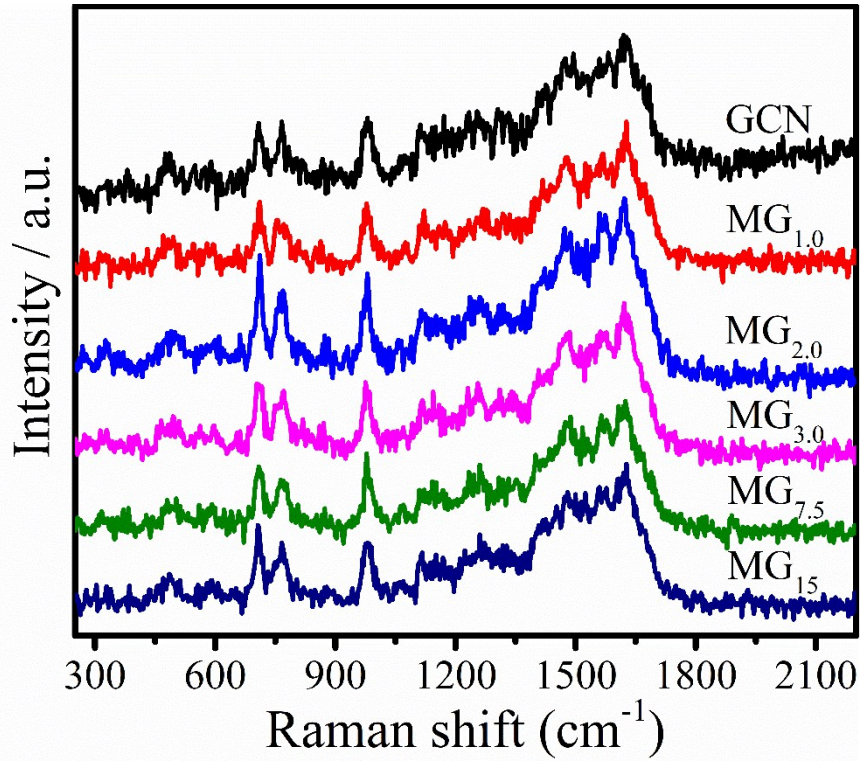


**Fig. S2** The UV-Raman spectra spectra for GCN and $MG_x$ ($x$ = 1.0, 2.0, 3.0, 7.5, 15)

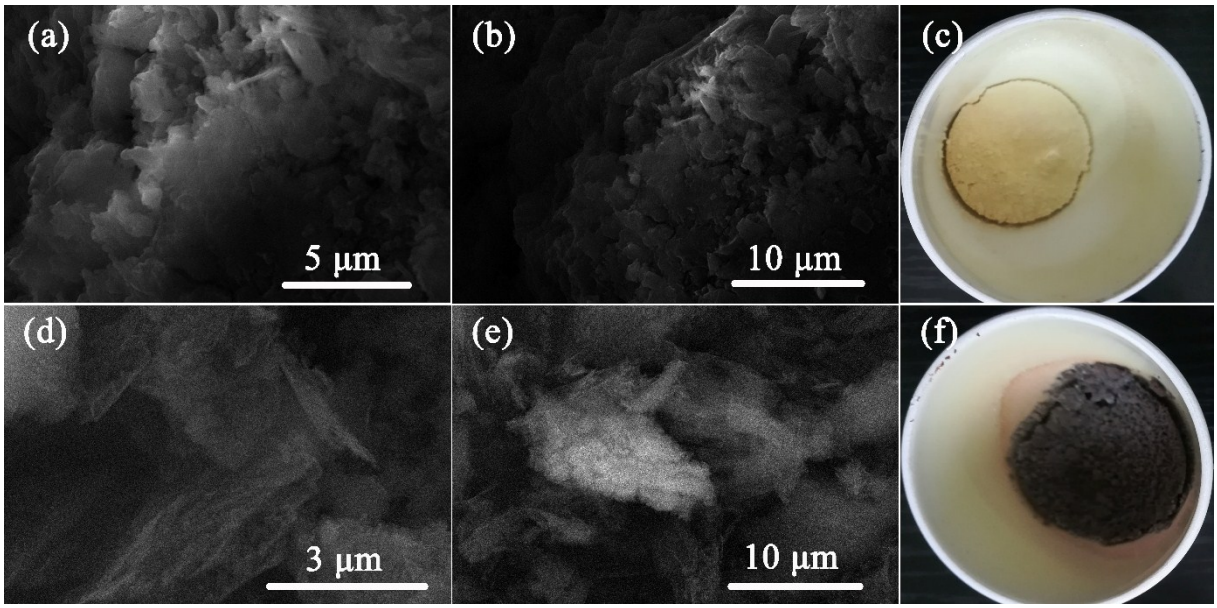


**Fig. S3** (a-b) SEM images of GCN, (c) The photo of GCN samples; (e-d) SEM images of $MG_{3.0}$, (f) The photo of $MG_{3.0}$ samples.

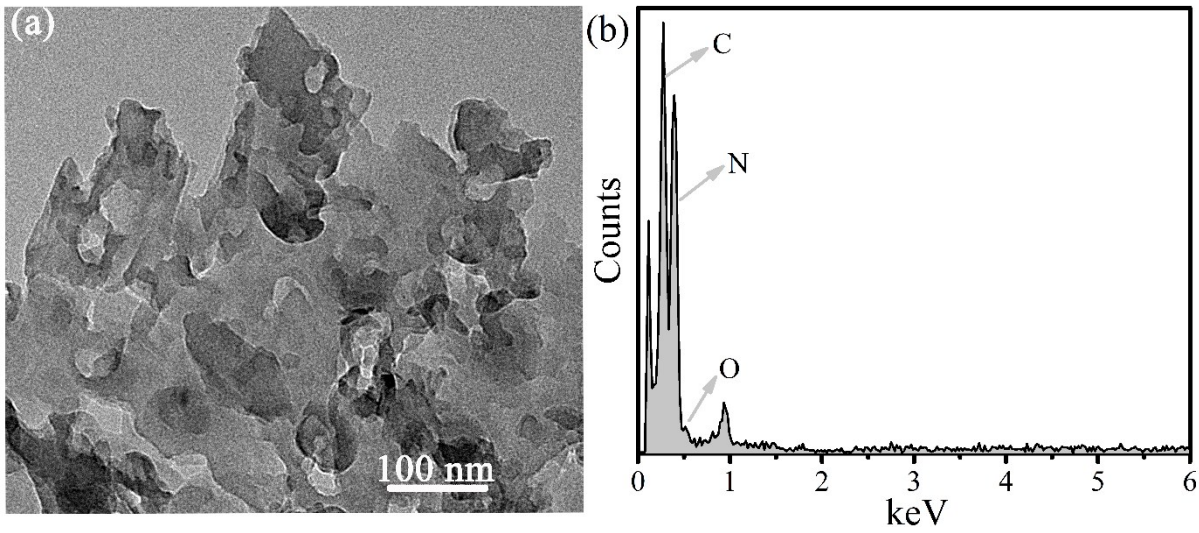


**Fig. S4** (a) TEM images of carbon nitride nanosheet $MG_{3.0}$ along with the energy-dispersive X-ray (EDX) spectrum.

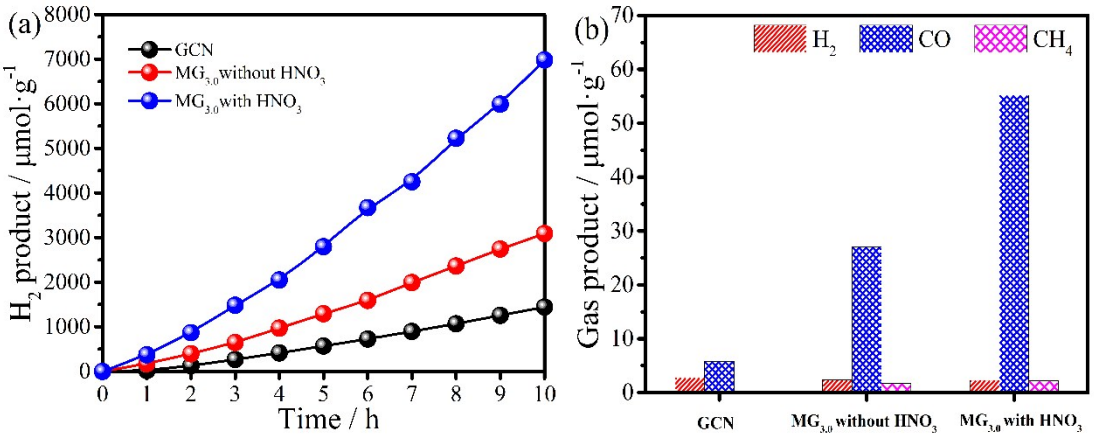


**Fig. S5** (a) $H_2$ evolution for GCN, $MG_{3.0}$ without $HNO_3$ treatment, $MG_{3.0}$ with $HNO_3$ treatment; (b) $CO_2$ reduction for GCN, $MG_{3.0}$ without $HNO_3$ treatment, $MG_{3.0}$ with $HNO_3$ treatment.

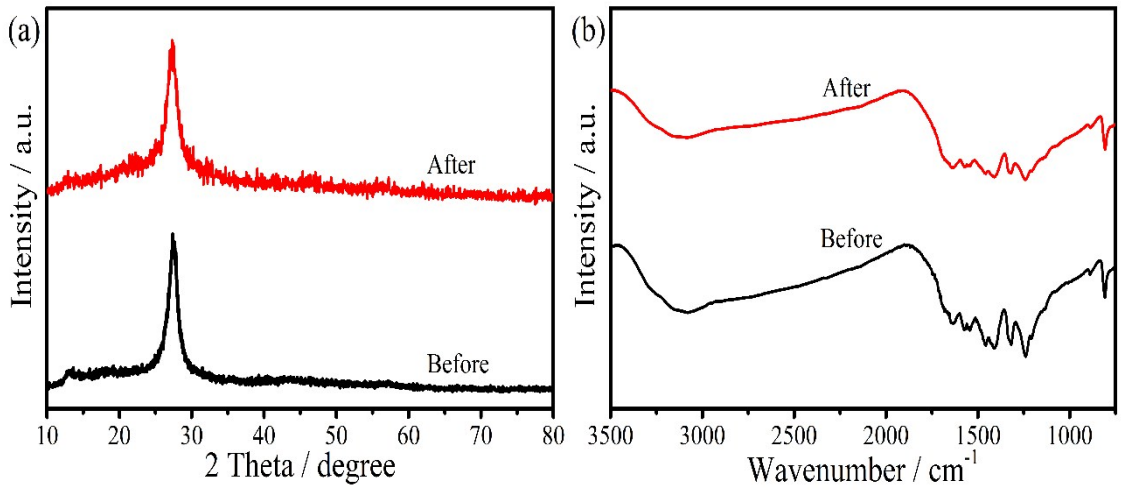


**Fig. S6** (a) XRD patterns and (b) FTIR spectra of $MG_{3.0}$ before and after the photocatalytic $H_2$ generation.

**Table S1** Elemental contents and C/N atomic ratio of GCN and $MG_{3.0}$ by elemental analyzer.

| Samples | N (wt %) | C (wt %) | C/N |
|---|---|---|---|
| **GCN** | 60.274 | 35.781 | 0.693 |
| **$MG_{3.0}$** | 57.083 | 37.547 | 0.767 |

**Table S2** Comparison of $H_2$ evolution rate for the carbon nitride nanosheet and reported carbon nitride base photocatalysts.

| Photocatalyst | HER / μmol·g$^{-1}$·h$^{-1}$ | Catalyst dose / mg | Cocatalyst dose | Reaction solution | Light source | References |
|---|---|---|---|---|---|---|
| **$MG_{3.0}$** | 698.4 | 30 | 3wt% Pt | 90 mL $H_2O$ & 10 mL TEOA | 300 W Xe lamp (>420 nm) | This work |
| **g-$C_3N_4$ nanosheet** | 646 | 50 | 1wt% Pt | 72 mL $H_2O$ & 8 mL lactic acid | 12 W LED (420 nm) | 1 |
| **CCN-1** | 529 | 100 | 3wt% Pt | 90 mL $H_2O$ & 10 mL TEOA | 300 W Xe lamp (>420 nm) | 2 |
| **5 wt% g-PAN/g-$C_3N_4$** | 370 | 100 | 1.5wt% Pt | 270 mL $H_2O$ & 30mL TEOA | 300 W Xe lamp (> 400 nm) | 3 |
| **20%BM/CNNs** | 563.4 | 100 | 3 wt% Pt | 90 mL $H_2O$ & 10 mL TEOA | 300 W Xe lamp (> 420 nm) | 4 |
| **TSCN** | 630 | 40 | 3 wt% Pt | 80 mL $H_2O$ & 10 mL TEOA | 300 W Xe lamp (> 420 nm) | 5 |
| **$CN\text{-}I_{1.0}$** | 760 | 50 | 3wt% Pt | 90 mL $H_2O$ & 10 mL TEOA | 300 W Xe lamp (> 420 nm) | 6 |
| **$CN\text{-}S_{2.0}$** | 650 | 50 | 3wt% Pt | 90 mL $H_2O$ & 10 mL TEOA | 300 W Xe lamp (> 420 nm) | 7 |
| **10 wt% $In_2O_3$/g-$C_3N_4$** | 197.5 | 5 | 0.5wt% Pt | 10 mL $H_2O$ containing 0.1 M L-ascorbic acid | 300 W Xe lamp (> 420 nm) | 8 |
| **CNF-0.5** | 127.5 | 100 | 3wt% Pt | 90 mL $H_2O$ & 10 mL TEOA | 500 W HBO lamp (> 420 nm) | 9 |

| | | | | | | |
|---|---|---|---|---|---|---|
| **CN-20/0D-ZnO** | 322 | 100 | 1wt% Pt | 90 mL $H_2O$ & 10 mL TEOA | 300 W Xe lamp (> 420 nm) | 10 |
| **Ce-CN-5** | 292.5 | 50 | 1wt% Pt | 180 mL $H_2O$ & 20 mL TEOA | 300 W Xe lamp (> 420 nm) | 11 |
| **GCNS** | 100 | 100 | 3wt% Pt | 90 mL $H_2O$ & 10 mL TEOA | 300 W Xe lamp (> 420 nm) | 12 |

**Section S1** The procedure to achieve the valence band potential ($E_{VB}$) and conduction band potential ($E_{CB}$) values.

The empirical equations of the $E_{VB}$ and $E_{CB}$ of a semiconductor material,

$$E_{VB} = \chi - E_e + 0.5E_g;\ E_{CB} = E_{VB} - E_g,$$

where $\chi$ is the absolute electronegativity of carbon nitride semiconductor, which is the geometric average of the absolute electronegativity of the constituent atoms (≈4.55 eV). $E_e$ is the energy of free electrons on the hydrogen scale (≈4.5 eV), and $E_g$ is the band gap energy of the semiconductor.

**Section S2** The discussion for the preferential formation of CO in the photocatalytic $CO_2$ reduction.

As we all know, photocatalytic $CO_2$ reduction to different products (e.g., CO, $CH_4$, HCOOH, $CH_3OH$, $CH_3CH_2OH$, etc.) requires different reduction potentials as listed in equations (1-5) [13-14]. Noted that the reduction potentials can be comparable to the proton reduction (6) and are less negative than the conduction band potential of carbon nitride. It seems to be that these reactions are feasible.

$$CO_2 + 2e^- + 2H^+ \rightarrow CO + H_2O \qquad E^0_{redox} = -0.53\,V \qquad (1)$$

$$CO_2 + 2e^- + 2H^+ \rightarrow HCOOH \qquad E^0_{redox} = -0.61\,V \qquad (2)$$

$$CO_2 + 6e^- + 6H^+ \rightarrow CH_3OH + H_2O \qquad E^0_{redox} = -0.38\,V \qquad (3)$$

$$CO_2 + 8e^- + 8H^+ \rightarrow CH_4 + 2H_2O \qquad E^0_{redox} = -0.24\,V \qquad (4)$$

$$2CO_2 + 12e^- + 9H_2O \rightarrow C_2H_5OH + 12OH^- \qquad E^0_{redox} = -0.33\,V \qquad (5)$$

$$2H^+ + 2e^- \rightarrow H_2 \qquad E^0_{redox} = -0.41\,V \qquad (6)$$

However, $CO_2$ reduction is a proton-assisted transfer of multiple electrons, involving a series of elementary reaction steps. For example, the pathway for $CO_2$ reduction to methane ($CH_4$) involves eight elementary reaction steps as listed in equations (7-14) [15].

$$CO_2 + e^- \rightarrow \cdot CO_2^- \qquad (7)$$

$$\cdot CO_2^- + e^- + H^+ \rightarrow CO + OH^- \quad (8)$$

$$CO + e^- \rightarrow \cdot CO^- \quad (9)$$

$$\cdot CO^- + e^- + H^+ \rightarrow C + OH^- \quad (10)$$

$$C + e^- + H^+ \rightarrow \cdot CH \quad (11)$$

$$\cdot CH + e^- + H^+ \rightarrow CH_2 \quad (12)$$

$$CH_2 + e^- + H^+ \rightarrow \cdot CH_3 \quad (13)$$

$$\cdot CH_3 + e^- + H^+ \rightarrow CH_4 \quad (14)$$

## REFERENCES


1 X. H. Wu, D. D. Gao, H. G. Yu, J. G. Yu, *Nanoscale*, 2019, DOI: 10.1039/c9nr00887j.

2 H. L. Li, F. P. Li, Z. Y. Wang, Y. C. Jiao, Y. Y. Liu, P. Wang, X. Y. Zhang, X. Y. Qin, Y. Dai, B. B. Huang, *Appl. Catal. B: Environ.*, 2018, **229**, 114-120.

3 F. He, G. Chen, Y. G. Yu, S. Hao, Y. S. Zhou, Y. Zheng, *ACS Appl. Mater. Interfaces*, 2014, **6**, 7171-7179.

4 J. Li, Y. C. Yin, E. Z. Liu, Y. N. Ma, J. Wan, J. Fan, X. Y. Hu, *J. Hazard. Mater.*, 2017, **321**, 183-192.

5 Z. W. Tong, D. Yang, Z. Li, Y. H. Nan, F. Ding, Y. C. Shen, Z. Y. Jiang, *ACS Nano,* 2017, **11**, 1103-1112.

6 G. G. Zhang; M. W. Zhang, X. X. Ye, X. Q. Qiu, S. Lin, X. C. Wang, *Adv. Mater.* 2014, **26**, 805-809.

7 J. S. Zhang, M. W. Zhang, G. G. Zhang, X. C. Wang, *ACS Catal.* 2012, **2**, 940-948.

8 S. W. Cao, X. F. Liu, Y. P. Yuan, Z. Y. Zhang, Y. S. Liao, J. Fang, S. C. J. Loo, T. C. Sum, C. Xue, *Appl. Catal. B: Environ.* 2014, **147**, 940-946.

9 Y. Wang, Y. Dai, M. Antonietti, H. R. Li, X. F. Chen, X. C. Wang, *Chem. Mater.* 2010, **22**, 5119-5121.

10 J. Wang, Y. Xia, H. Y. Zhao, G. F. Wang, L. Xiang, J. L. Xu, S. Komarneni, *Appl. Catal. B: Environ.*, 2017, **206**, 406-416.

11 J. Chen, S. H. Shen, P. Wu, L. J. Guo, *Green Chem.*, 2015, **17**, 509-517.

12 X. C. Wang, K. Maeda, A. Thomas, K. Takanabe, G. Xin, J. M. Carlsson, K. Domen, M. Antonietti *Nature*, 2009, **8**, 76-80.

13 N. M. Dimitrijevic, B. K. Vijayan, O. G. Poluektov, T. Rajh, K. A. Gray, H. He, P. Zapol, *J. Am. Chem. Soc.*, 2011, **133**, 3964-3971.

14 V. P. Indrakanti, J. D. Kubicki, H. H. Schobert, *Energy Environ. Sci.*, 2009, **2**, 745-758.

15 M. Anpo, H. Yamashita, Y. Ichihashi, S. Ehara, *J. Electroanal. Chem.*, 1995, **396**, 21-26.